
PERGAMON

Available at
www.ElsevierComputerScience.com
POWERED BY SCIENCE DIRECT®

Pattern Recognition 38 (2005) 559–576

PATTERN RECOGNITION
THE JOURNAL OF THE PATTERN RECOGNITION SOCIETY
www.elsevier.com/locate/patcog

Wavelet based methods on patterned fabric defect detection

Henry Y.T. Ngan[a], Grantham K.H. Pang[a,*], S.P. Yung[b], Michael K. Ng[b]

[a]*Department of Electrical and Electronic Engineering, Industrial Automation Research Laboratory, The University of Hong Kong, Pokfulam Road, Kowloon, Hong Kong*
[b]*Department of Mathematics, The University of Hong Kong, Pokfulam Road, Hong Kong*

Received 26 November 2003; received in revised form 25 June 2004; accepted 29 July 2004

Abstract

The wavelet transform (WT) has been developed over 20 years and successfully applied in defect detection on plain (unpatterned) fabric. This paper is on the use of the wavelet transform to develop an automated visual inspection method for defect detection on patterned fabric. A method called direct thresholding (DT) based on WT detailed subimages has been developed. The golden image subtraction method (GIS) is also introduced. GIS is an efficient and fast method, which can segment out the defective regions on patterned fabric effectively. In this paper, the method of wavelet preprocessed golden image subtraction (WGIS) has been developed for defect detection on patterned fabric or repetitive patterned texture. This paper also presents a comparison of the three methods. It can be concluded that the WGIS method provides the best detection result. The overall detection success rate is 96.7% with 30 defect-free images and 30 defective patterned images for one common kind of patterned Jacquard fabric.

Keywords: Patterned fabric inspection; Defect detection; Wavelet transform, Texture analysis; Patterned texture

1. Introduction

Cost reduction in production and inspection processes is an important objective for textile manufacturers. Yet, quality control is extremely important as well. In fabric defect inspection for both weaving fabrics and knitting fabrics, most inspection is conducted by human eyes. Usually, a human inspector would handle one manual visual inspection machine in a weaving mall and continuously inspect a number of fabric rolls. The cost for hiring those workers and the facilities setup is high. Human mistakes are frequent as well. Hence, the demand for automated inspection systems is great. Automated fabric inspection systems exist nowadays but they are expensive and are only for plain and twill fabrics, which are called the 'unpatterned' fabrics. Several major methods have been developed for "unpatterned" fabric [1–5]. These include Neural Network [6–8], Fourier Transform [9–13], Gabor filters [14–18] and the wavelet transform (WT) [19–26]. These methods have achieved a high detection success rate and some of them can recognize over 95% of defect on those plain and twill fabric.

However, very little research has been carried out on patterned fabric so far. One of the reasons is the difficulty and sophisticated design on patterned fabric. The 'patterned' fabric is defined as fabric with repetitive patterned units on its design. Under the class of 'patterned' fabric, there are still many categories. The aim of this research is to develop an effective way to detect defects on 'patterned' fabric, especially for Jacquard patterned fabric, where a flower or graphic logo may appear on the fabric. The repetitive unit can range from the simplest charter box, dots, to the most

* Corresponding author. Tel.: +852 2857 8492; fax: +852 2559 8738.
E-mail addresses: henryyan@graduate.hku.hk (H.Y.T. Ngan), gpang@eee.hku.hk (G.K.H. Pang).

0031-3203/$30.00
doi:10.1016/j.patcog.2004.07.009

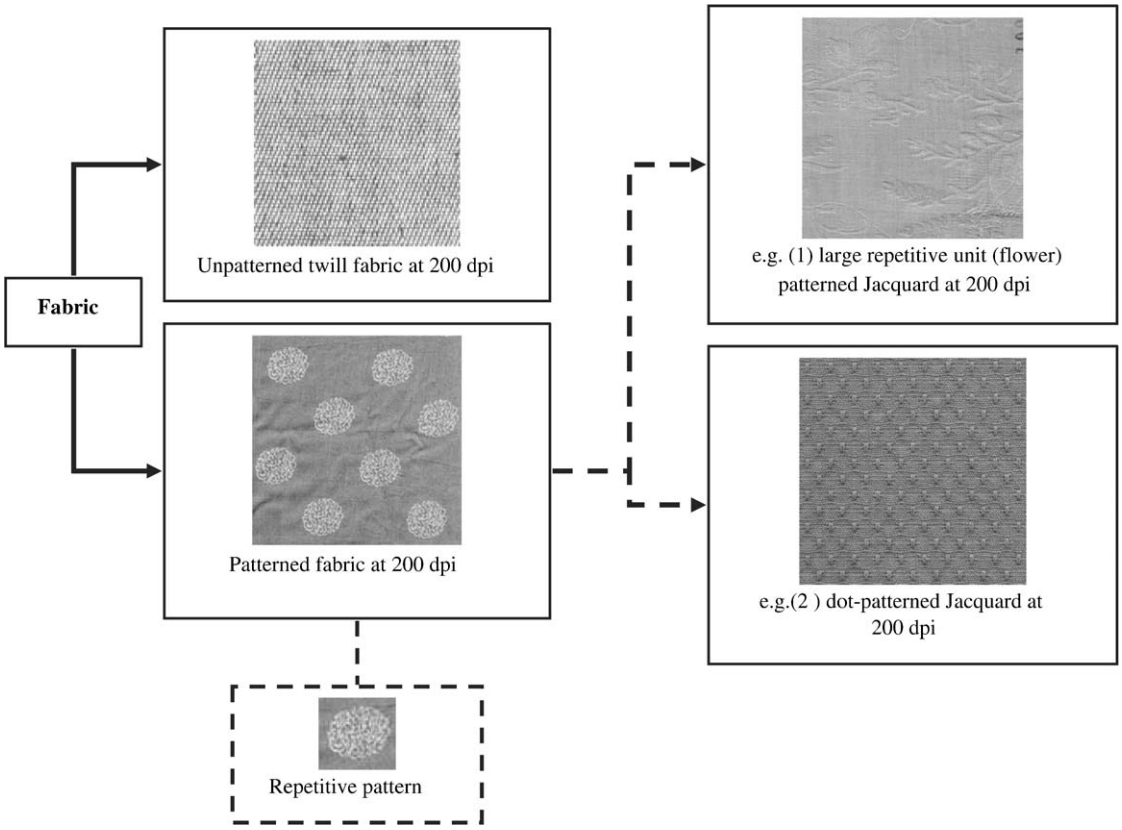

Fig. 1. Classification of fabric.

complicated multiple flowers, animals or designed patterns. Besides, there are lots of sub-categories under patterned fabric and Fig. 1 illustrates on a classification of fabrics.

Section 2 of this paper gives a literature review of prior defect detection methods on patterned fabrics. Then, the method of direct thresholding (DT) on detailed subimages is given in Section 3. Section 4 outlines the basic golden image subtraction (GIS) method. Then, Wavelet preprocessed golden image subtraction (WGIS) method will be presented in Section 5. A summary is presented in Section 6. Lastly, conclusions are given in Section 7.

2. Literature review and evaluation of defect detection methods on patterned fabrics

From a literature search, two categories of method for defect detection on patterned fabrics are found. They will be presented and evaluated with the use of a dot-patterned designed Jacquard, which is shown in Fig. 2. Six kinds of defects (broken end, holes, knots, netting multiple, oil stain and dirty yarn) are shown in Fig. 3. Oil stain is a discrete area of oil discoloration on a fabric while dirty yarn means one or several yarns are discolored by oil. The area of dirty yarn is usually smaller than oil stain. Histogram equalization has been performed on all images (e.g. see Fig. 4). All images for training and testing have 256 x 256 pixels in grey level scale.

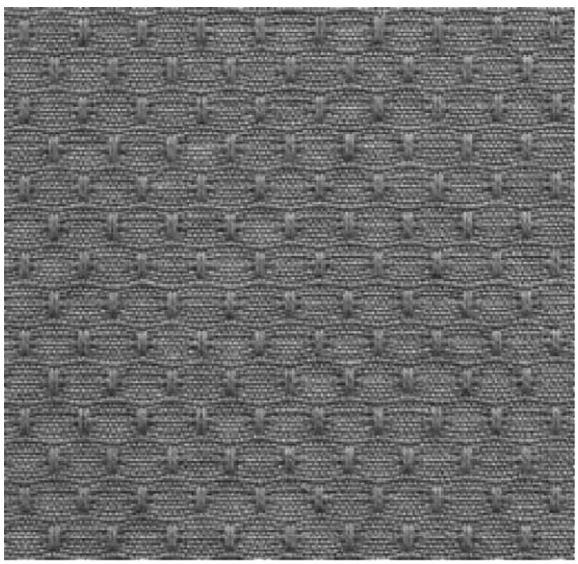

Fig. 2. Dot-patterned designed Jacquard.

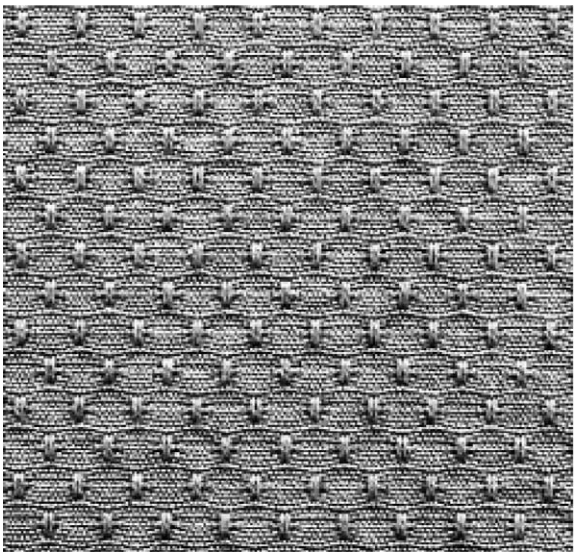

Fig. 3. Six type of histogram equalized defective patterned images with (a) broken end, (b) holes, (c) knots, (d) netting multiple, (e) oil stain and (f) dirty yarn.

2.1. The Hash function method

Baykal [27,28] suggested to use hash functions, originally which were developed from cryptography, for defect detection on patterned textures. The proposed stages of the method of hash functions are illustrated in Fig. 5. Four basic families of hash functions are suggested by Baykal et al. [27,28]: checksum (1), plain (2), XOR (3) and multiplication (4). The equations of them are given as follows:

$$Checksum\ type:\ h[x]=\sum_{y=1}^{N} I[x,y], \tag{1}$$

$$Plain\ type:\ h[x]=\sum_{y=1}^{N} I[x,y]\times W_r\left[\frac{y}{N}\right], \tag{2}$$

$$XOR\ type: h[x]=\sum_{y=1}^{N} I[x,y] \oplus \mathrm{E}\left[n \bmod \left(\frac{N}{(r+1)}\right)\right]\times W_r\left[\frac{y}{N}\right], \tag{3}$$

$$Multiplication\ type: h[x]=\sum_{y=1}^{N} I[x,y] \times \mathrm{T}\left[n \bmod \left(\frac{N}{(r+1)}\right)\right]\times W_r\left[\frac{y}{N}\right], \tag{4}$$

where $I[x,y]$ is the image matrix in $M\times N$, $W_r[t]$ is a Walsh function [29–31] of type r and E[] and T[] are periodic functions to be ex-ored or multiplied with the pixel values of the image. The Walsh function is defined as $W_r[t]=\prod_{i=1}^{k}[p_i(t)]^{\alpha_i}$ where the index n is given by the binary expansion $n=\alpha_1+\alpha_2 2^1+\cdots+\alpha_k 2^{k-1}$ and

$$\alpha_i=\begin{cases}0,1, & i\neq k,\\ 1, & i=k.\end{cases}$$

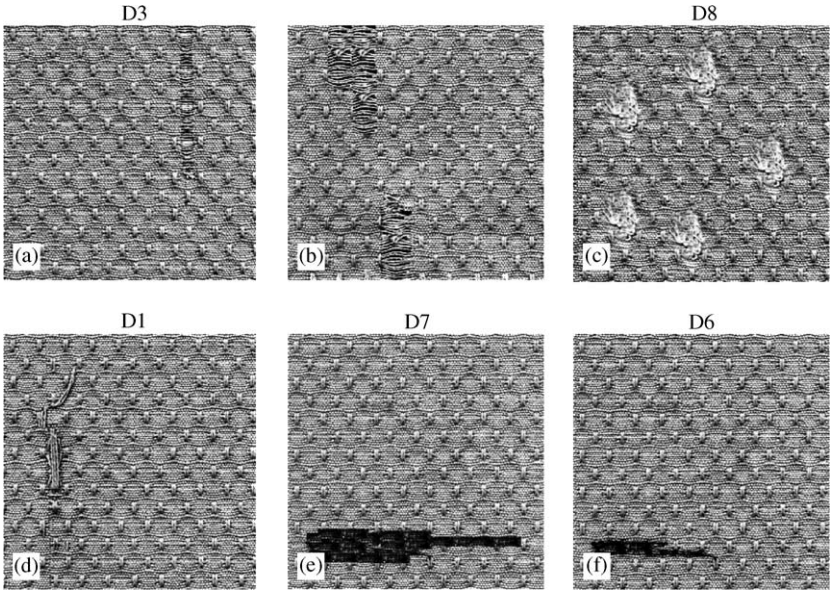

Fig. 4. After histogram equalization.

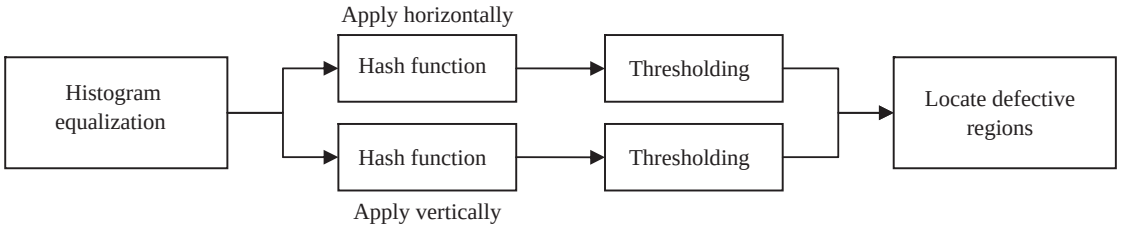

Fig. 5. The stages of the hash function method.

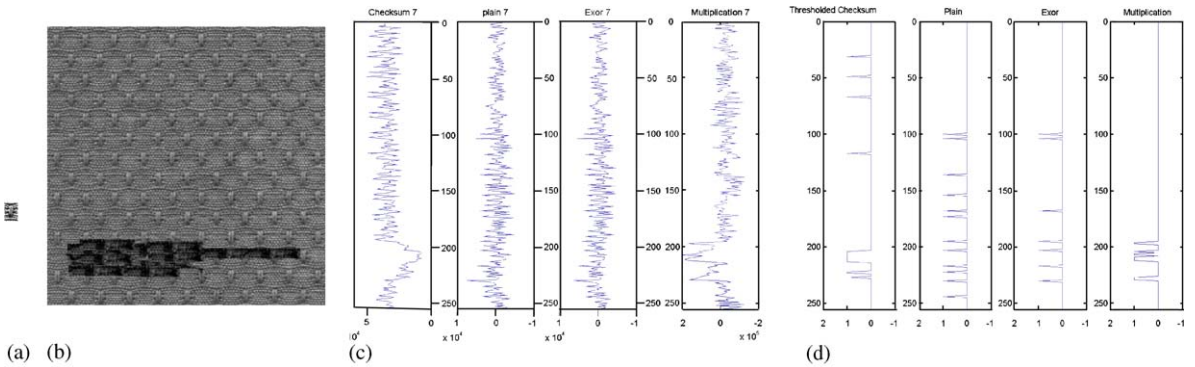

Fig. 6. (a) A repetitive unit of a defective patterned image with oil stain. (b) A histogram equalized reference image. (c) (From left to right) Signatures of checksum function, plain hash function$_{(r=3)}$, XOR function$_{(r=3)}$ and multiplication hash function$_{(r=4)}$ on rows. (d) Result of the signatures after thresholding.

$p_i(t)$ is called Rademacher function with

$$p_1(t+\eta) = p_1(t) = \begin{cases} +1, & 0 \leqslant t < \frac{1}{2}, \\ -1, & \frac{1}{2} \leqslant t < 1 \end{cases}$$

for any integer η and $p_k(t) = p_1(2^{k-1}t)$ for higher order. The hash function used Walsh function to make an off-set effect on the input values of an array on row or column. The choice of hash function type depends on the complexity of texture. For more complex patterned texture, high order type like Eqs. (3) and (4) may be chosen. For example, the checksum hash function (1) is just a sum of every horizontal line and does not give much information on small defect of large complex patterned fabric.

A simple way for detection on the dot-patterned fabric is using the number of periods of a test image. If it can be coincided with one particular type of Walsh function, a DT on the two signatures also enable detection of defects. This situation is shown in Fig. 6, which shows the signatures of checksum function, plain hash function, XOR hash function and multiplication hash function from the defect-free image, as the number of periods of the test image is tuned to match with the type of Walsh function. However, for some extreme cases, Baykal et al. [27] suggested to use a subtraction method. Every type of hash function generates two signatures (row and column) of a test image. They are then subtracted by the two signatures of a golden template of one repetitive unit from a reference image. Then, any unusual jump can be segmented out by thresholding.

For evaluation, 30 defect-free images (Fig. 4) and 30 defective patterned images (Fig. 3) have been used. From the use of the simplest Checksum hash function to the most complex multiplication hash function, the value of r for the Walsh function is required to be tuned in order to match the number of periods that can be traced on the test image. Hash function can be applied along the rows and the columns. Therefore, there are a total of eight signatures (row and column) from all four types of hash functions. Every signature is bounded by an upper bound and lower bound within a range in the defect-free images if the period of images coincides with the Walsh function. So, the averaged upper bound and averaged lower bound for all signatures, $[t_{tower}, t_{upper}]$, are the threshold values. The thresholding is defined as follows,

$$T(i) = \begin{cases} 0 & t_{lower} \leqslant i \leqslant t_{upper}, \quad \text{for } i\text{th row.} \\ 1 & \text{otherwise,} \end{cases}$$

In this paper, all four types of hash functions have been implemented and tested. As suggested by Baykal [27,28], the results from using the multiplication hash function has given the best result among the different types of hash functions in the evaluation. Fig. 7 gives the results of threshold

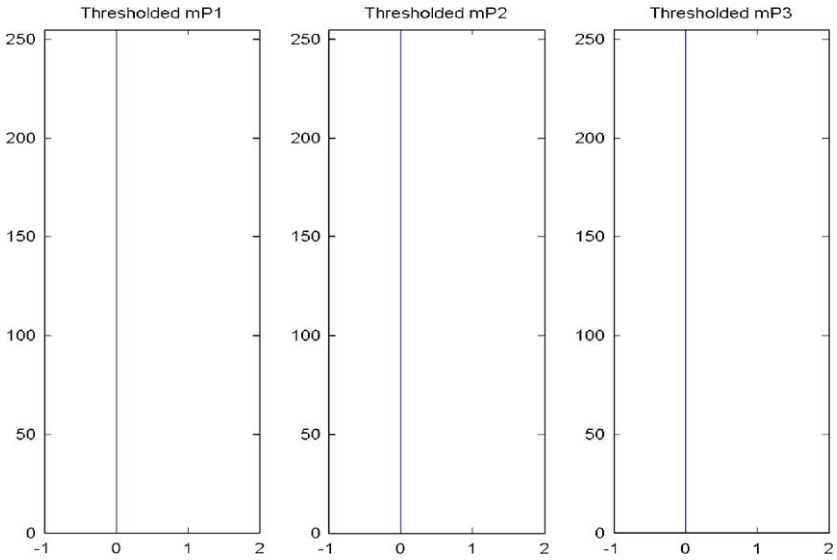

Fig. 7. Threshold signatures of multiplication hash function for three defect-free images.

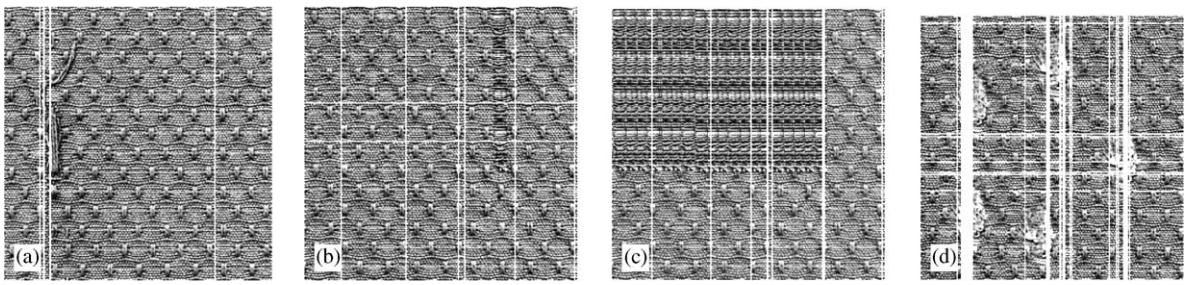

Fig. 8. Four typical defective patterned images examples of misclassification with threshold signatures of multiplication hash function presented on defective patterned images (detected on horizontal side and vertical sides).

signatures of multiplication hash function for three defect-free images. They have been correctly detected as having no defects. However, not all defects can be successfully segmented out by the multiplication hash function. For example, in Fig. 8, Netting Multiple and Broken End are misclassified on the right side and left side respectively. Broken End 2 cannot be fully detected in column detection and a large portion of its defective regions is not covered by thresholding results. There are no successful row detection on Netting Multiple and Knots in Fig. 8(a) and (d). Furthermore, the hash function is required to be fine tuned for the corresponding number of periods on more sophisticated patterned texture in order to generate a good result. Therefore, the hash function method is not very effective and still has a lot of room for improvement.

On the other hand, Thomas and Cattoen [32] suggested to use the image block densitometrical profile to analyse the average value of each row or each column in the test image. The idea is similar to the hash function method of Baykal et al. [27,28]. In fact, the image block densitometrical profile of Thomas's design is the same as the checksum hash function defined by Baykal. One advantage of the hash function is time-saving because the image is treated as one dimensional array. The weakness of hash function is its sensitivity to noise and its inability in outling the shape of defect after detection.

2.2. The traditional image subtraction (TIS) method

Chin and Harlow [33] have (Fig. 9) tried to use exclusive or operation as image subtraction method on traditional defect inspection of PCBs (Fig. 10). This involves the subtraction of an entire image of test circuit board from a whole perfect master image of the same type of circuit board. Later on, for patterned fabric defect detection, Li et al. [34], Sandy et al. [35] suggested to use the same technique as Chin on

Fig. 9. The stages of the TIS method.

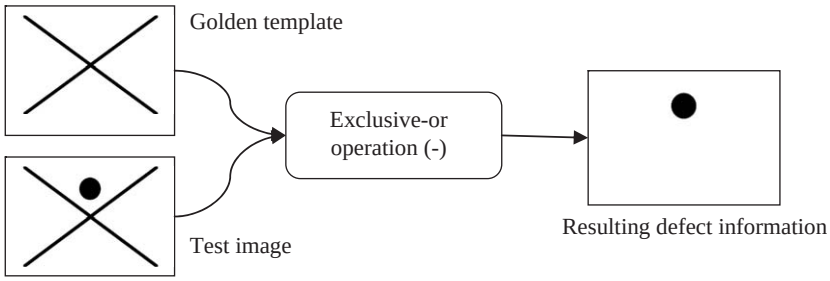

Fig. 10. Exclusive-or operation in traditional image subtraction.

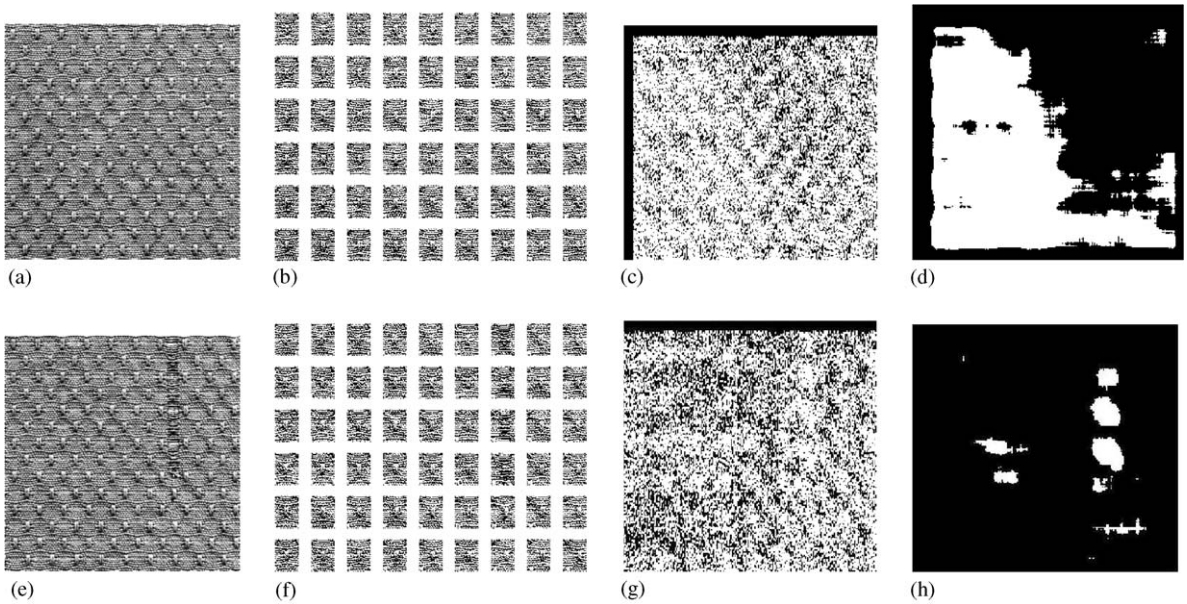

Fig. 11. (a) A defect-free image and (e) A defective patterned image with broken end, (b) and (f) partitions of (a) and (e) resp., (c) and (g) results of TIS of (b) and (f) resp., (d) and (h) filtered images of (c) and (g) resp.

Lace, which is one kind of patterned fabric with fine and complex pattern of threads. The subtractions on Lace are based on a prototype version and a test version in same pattern. They used autocorrelation function to find the repeat pattern distance of Lace and undergo partitioning on every test Lace image. Then, there will be image subtractions for every partition. (Fig. 11) Thresholding and neural network techniques are applied on those results in order to classify the defects. However, this method is weak due to the distortion of Lace components.

3. Method of direct thresholding on detailed subimages

The method of DT on detailed subimages is illustrated in Fig. 12. In this section, the evaluation results show the use of the WT as a segmentation tool for defect detection on patterned fabrics. For implementation, 30 defect-free images and 30 defective patterned images, same as Figs. 3 and 4, have been used in Section 2. The images are input in size of 256×256 pixels with 8-bit gray levels and they are all processed with histogram

Fig. 12. Steps of method of DT on detailed subimages.

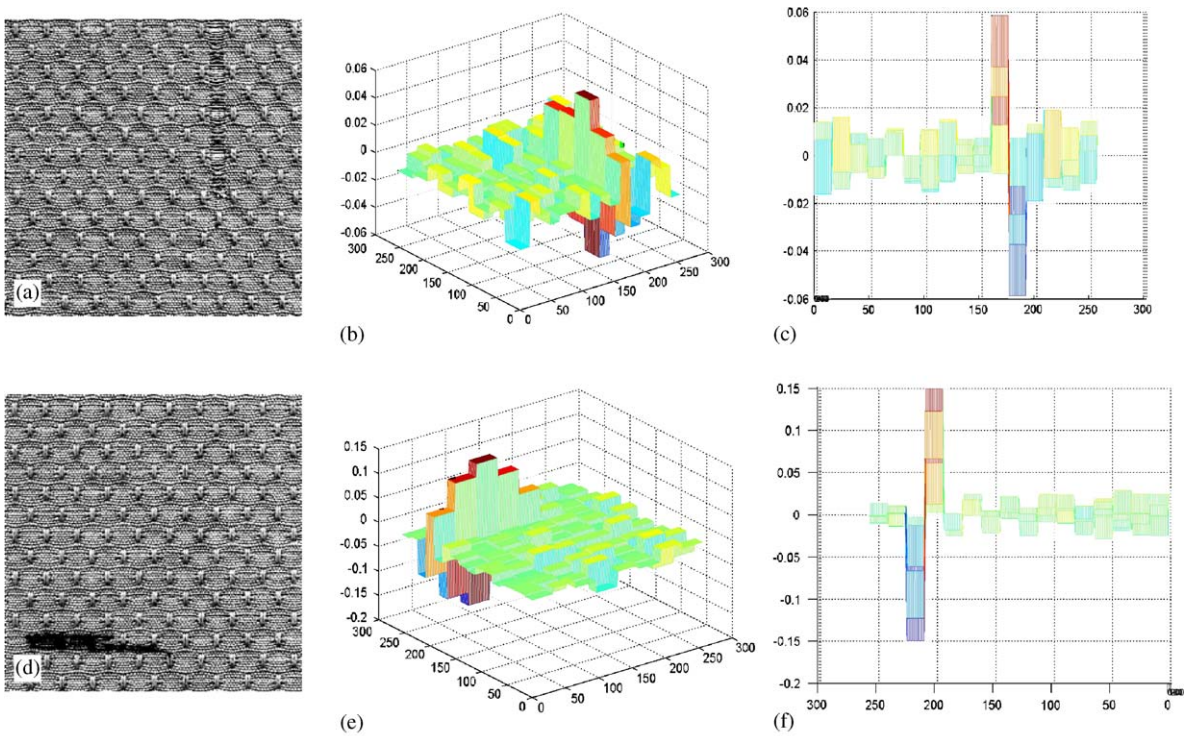

Fig. 13. Histogram equalized defective patterned image with (a) broken yarn, (b) oil stain (b), (e). Diagonal view and (c), (f) Longitudinal view of fourth level vertical and horizontal detail after Haar wavelet decomposition respectively.

equalization. Haar wavelet type is chosen in WT due to its simplicity.

In this method, WT is performed using Haar wavelet filter coefficients and the length of decomposition filter is two. The input images are decomposed into level four in order to obtain the best result for detection and keep an appropriate resolution. If a higher level is used, the result would be too coarse for defect analysis. By selecting an appropriate level of detailed images, the Haar WT can show up a significant detection result. The non-defective region would be suppressed down and the defective region would be enhanced, e.g., Fig. 13 (two examples are shown).

3.1. The procedures of the direct thresholding (DT) method

1. Use three reference images for Haar wavelet decompositions.
2. Extract the corresponding fourth level horizontal and vertical details.
3. Obtain the lower and upper bound among all pixel values of each detailed image for the threshold values.
4. Here, we assume that certain degree of white Gaussian noise should appear in each processed image since each original image has imperfections as fabric yarns contains dirt and impurities. Hence, we would like to reduce the threshold values so as to let some white pixels to appear in the processed image of the reference fabrics in our investigation. The initial noise level is assumed as 3%. The new threshold values should be $[0.97{*}t_{lower,i}, 0.97{*}t_{upper,i}]$ for each detail i where t_{lower} is negative value and t_{upper} is positive. By doing so, the range of thresholding is contracted and some white pixels would appear.
5. Average the lower and upper bound values of the three horizontal details in level 4 and do the same process for vertical details.

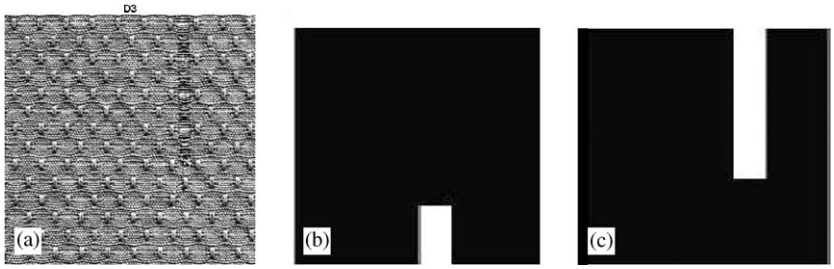

Fig. 14. (a) Defective patterned image with broken end, (b) thresholded images of horizontal details and (c) vertical details at level 4 using average threshold values with noise level 3%.

Fig. 15. Or-operation of horizontal and vertical details in level 4 for each defect-free image, P1, P2 and P3 (left to right), assuming 3% noise initially.

6. Use the average values to test 30 defect-free images and 30 defective patterned images (The result of a defective patterned image with broken end is shown in Fig. 14).
7. Perform an Or-operation of horizontal and vertical details on the fourth level.
8. Apply smoothing filter to remove the noise after the or-operation (Figs. 15 and 16).

3.2. Detection success rate on 60 samples using the DT method

In the initial evaluation, the noise level has been set at 3% and the decomposition level of Haar wavelet transform is four. For a 16×16 final image from the fourth level Haar wavelet decomposition, 8 white pixels out of 256 are set as threshold for defective patterned image. Twenty-six of 30 defect-free images were shown less than 8 pixels after filtering and 27 of 30 defective patterned images could be correctly detected. The detection success rates are 86.77% for defect-free images and 90% for defective patterned images. Then, the overall detection success rate is 88.3%.

3.3. Effect due to varying the range of thresholding for detection

It is interesting to find that with 10% noise level assumption, all defective patterned images could be correctly detected. Suppose the term "false positive" is used to describe a defect-free image with detected defects where none exists. Then, all 30 defect-free images have been "false positive" as there is too much noise in the final filtered image as illustrated in Fig. 17. For 3% noise level, the false positive rate for 30 defect-free and 30 defective patterned images are 13.3% and 10%, respectively. Therefore, the initial noise level should be adjusted to 3% to avoid high false positive rate.

3.4. Effect due to decomposition level for detection

Due to multi-resolution property in the WT, $m+1$th level detail will have a lower resolution than m level. It has been found that good detection result is obtained at level 4. For the level four Haar WT, the detail of the fourth level is of resolution 16 x 16 blocks. Hence, any defect should be larger than or around 16×16 pixels in the original defective patterned image. For defects with size smaller than 16×16 pixels, the defects may not be detected successfully.

3.5. Effect due to selecting different detailed subimages

One may wonder why diagonal detail is discarded in the method of DT on detailed subimages. In our evaluation, fourth level diagonal detail has also been considered and it was thresholded and followed by an or-operation. (Fig. 12) Then, 24 of 30 defect-free images (80%

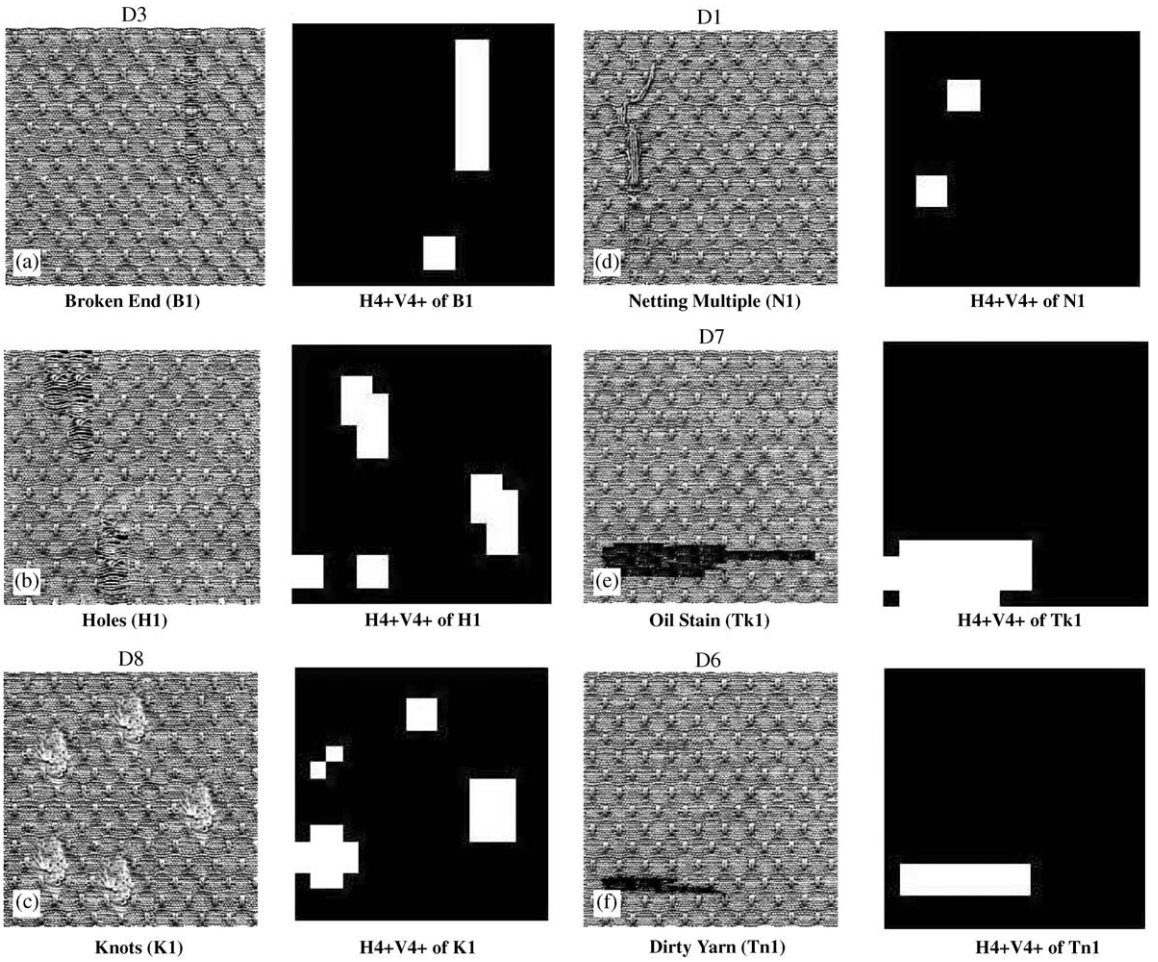

Fig. 16. Filtered of or-operated details in level 4 for each type of defective patterned image (broken end, holes, knots, netting multiple, dirty yarn and oil stain), assuming 3% noise initially.

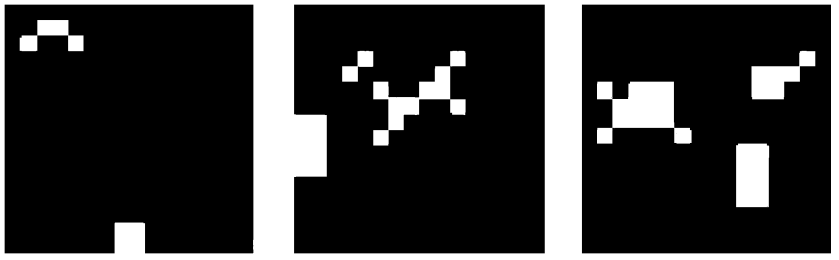

Fig. 17. Or-operation of horizontal and vertical details in level 4 for each defect-free image, P1, P2 and P3 (left to right) ,assuming 10% noise initially.

detection success rate) and 28 of 30 defective patterned images (96.67% detection success rate) are correctly detected. Compared with using only horizontal and vertical details, the detection success rate for defect-free images is much lower. It has caused a high false alarm rate in our evaluation.

3.6. Effect due to exchanging the last two steps

Method A of Fig. 18 is currently used in this section. The reason for using method A is that it can retain much information by processing the or-operation before smooth filtering. Hence, a higher detection success rate has been

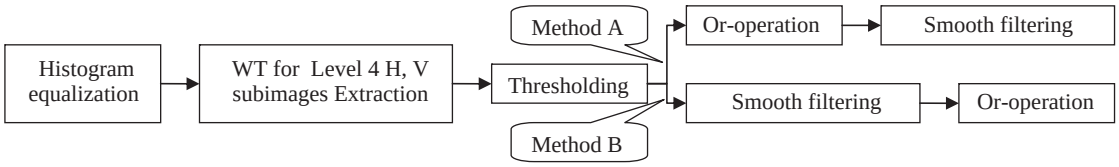

Fig. 18. Exchanging last two steps of method of DT on detailed subimages.

obtained by method A. If method B is applied, 24 of 30 defect-free images (80% detection success rate) and 28 of 30 defective patterned images (93.33% detection success rate) have been correctly detected. So, there has been a higher false positive rate in method B compared with method A, which successfully detect 26 defect-free images and has 88.3% overall detection success rate. It is believed that useful information such as defect location has been eliminated by the smoothing process in method B.

4. Basic golden image subtraction method

The basic GIS method is designed for detecting defects on patterned fabric. The stages of the basic GIS method are described in Fig. 19. Our GIS method is different from Chin and Harlow [33] since our golden template can contain several repetitive units taken from the defect-free image. Also, the golden image used in GIS is similar to the use of a convolution filter on test image, and it is not a static comparison between the golden template and the test image. The major drawback of the traditional method is that it cannot match perfectly pixel to pixel between the test area and the golden template. However, the method of GIS does not have this weakness.

First of all, the input images will undergo histogram equalization to enhance the contrast. Then, the ideas of the basic GIS method are described for defect detection on a type of patterned fabric, which is a dot-patterned designed Jacquard. The basic GIS method is applied on the test images. After GIS, a thresholding process will be performed and this section gives a discussion of how the thresholding value is obtained from the training samples. After that, this section describes how the noise is removed by the median filter or Wiener filter.

4.1. Definition of the energy of golden image subtraction

If any $m \times n$ size subtracted image $H_{xy} = H_{xy}(i, j) = (h_{ij})$ from test patterned image P is subtracted from a golden image $G = (g_{ij})$ with size of $m \times n$ pixels (larger than one repetitive unit) from that reference patterned image F with size of $M \times N$, then the energy of GIS is defined by

$$R = (r_{xy}) = \frac{1}{mn} \sum_{i=1}^{m} \sum_{j=1}^{n} \left| g_{ij} - h_{ij} \right|, \tag{5}$$

where $x = 1, \ldots, M - m + 1$, and $y = 1, \ldots, N - n + 1$, $i = 1, \ldots, m$ and $j = 1, \ldots, n (0 < n \leqslant N, 0 < m \leqslant M)$.

4.2. The procedures of the golden image subtraction (GIS) method (Fig. 20)

1. Obtain a golden image $G = (g_{ij})$ of size $m \times n$ pixels (larger than one repetitive unit) from a reference patterned fabric image F of size $m \times n$ (Fig. 20).
2. Perform the subtractions between the golden image $G = (g_{ij})$ of size $m \times n$ pixels and the subtracted image $H_{xy} = H_{xy}(i, j) = (h_{ij})$ of same size, by the definition of energy of GIS, on the test image P from the first pixel to $M - m + 1$th pixel of first row and go through second row, and so on until $N - n + 1$th row.
3. Return a $(M - m + 1)x(N - n + 1)$ matrix, which is defined as a resultant image, $R = (r_{xy})$ by the energies of GIS.

4.3. Thresholding

For a reference image (Fig. 21(a)), periodic hills and valleys will appear on the plot from the resultant image R (Fig. 21(c) and (d)). A threshold image $U = (u_{ij})$ is defined as

$$u_{ij} = \begin{cases} 1 & \text{if} \quad r_{ij} > T, \\ 0 & \text{if} \quad r_{ij} \leqslant T, \end{cases}$$

where $i = 1, \ldots, M - m + 1$ and $j = 1, \ldots, N - n + 1$, where r_{ij} is the energy value of resultant image R. T is the moderate threshold value. This image can be considered as a binary image and give the information on defects. A direct way to obtain the threshold value is to select the peak value of the hills from R of a reference image. For the defective samples, subtractions on the defective area will cause a distinguish jump that is quite different from the normal level (Fig. 21 (e) and (f)). Hence, it will outline the defective region if an appropriate threshold value is used. Therefore, a training stage for obtaining the threshold value is essential.

The method to train the threshold value is first to collect a large amount of reference samples F_k where $k = 1, \ldots, w$,

Fig. 19. The stages of the basic GIS method.

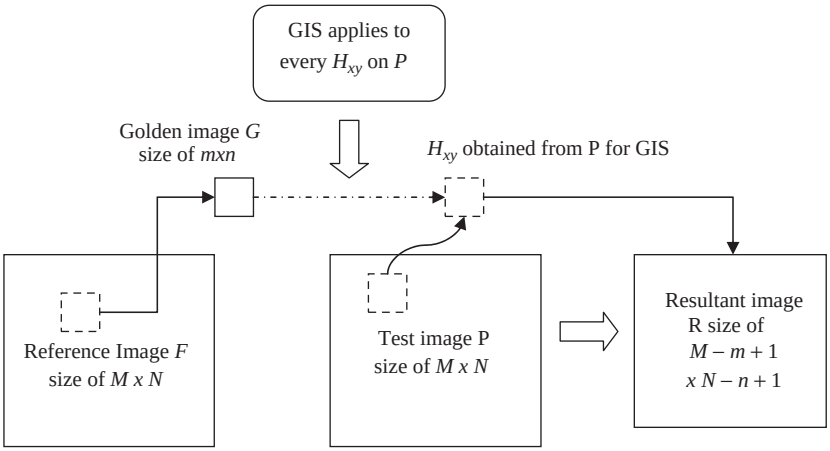

Fig. 20. Idea of the basic GIS method.

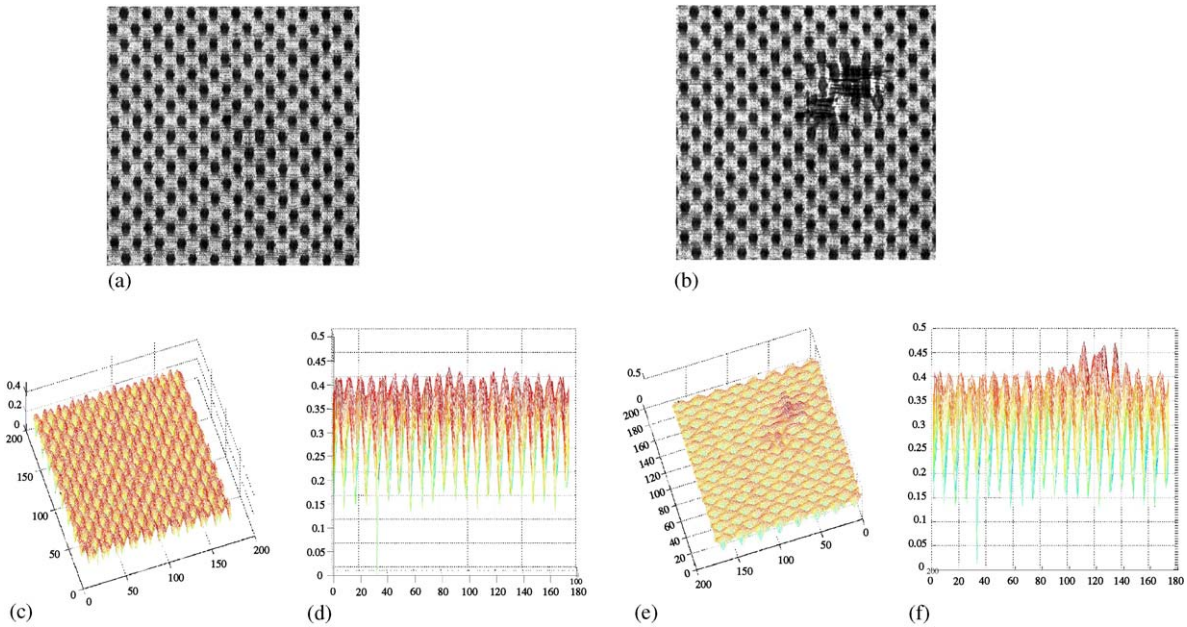

Fig. 21. (c), (e) the overhead views and (d), (f) longitudinal views for a reference sample (a) and a defective patterned image (b), of resultant matrix R after GIS respectively.

i.e. w reference samples. Using the same golden image, GIS is applied on every sample. So, if $T_k = \max(r_{xy})$ where $x = 1, \ldots, M-m+1$ *and* $y = 1, \ldots, N-n+1$, the maximum value of energy of GIS of every reference sample for $k = 1, \ldots, w$, is used as an indicator, then the defective regions are segmented out. A noise tolerance is given so that we would truncate the highest portion for each T_k. For example, the T_k can be 0.95 of the original peak value in R_k if there is a 5% noise. Afterward, averaging all the maximums $(T_1 T_2, \ldots, T_w)$ will give us the moderate threshold

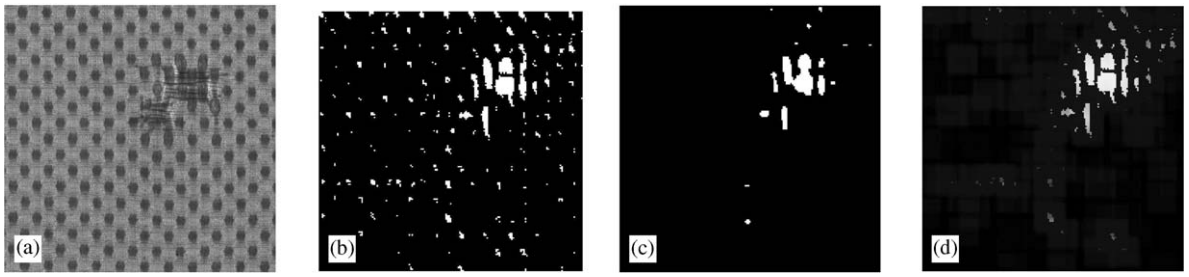

Fig. 22. (a) Test defective pattern sample in Fig. 12(b), (b) thresholded image, (c) using median filter on thresholded image, (d) using Wiener filter on thresholded image.

value T, where $T = (T_1 + T_2 + \cdots + T_w)/w$. Using this threshold value, the defective region can be found on a test image P. Fig. 22(a) and (b) illustrates a thresholded image with a moderate threshold value T.

4.4. Smooth filtering process

As mentioned above, there will be some white impulse noise when the resultant image is thresholded. So, we need to apply filtering techniques on threshold image D in order to remove the noise and enhance the image for defect on D. After trying several types of filters, two filters are chosen to achieve that goal. One is median filter [36] and the other one is Wiener filter [36]. Median filter is effective in dealing with bipolar and unipolar impulse noise. Wiener filter is one kind of inverse filters for degradation image. With the help of appropriate filters, the result of threshold image D would be improved to an appreciated level. Fig. 22(c) and (d) give the results from the threshold image.

5. Results and discussion

Thirty defect-free images (Fig. 4) and 30 defective patterned images (Fig. 3) have been used. The size of the golden image is of dimension 47×40, which is approximately equivalent to five repetitive units in the dot-patterned designed Jacquard, for GIS. All defect-free images were correctly detected. The final results are shown in Fig. 23 for defective patterned images. In Fig. 23(b), (e) and (f), the defective regions H1, Tk1 and Tn1 could be shown after thresholding and smooth filtering. It should be noted that holes (H1) are defects of large area, and dirty yarn (Tn1) and oil stain (Tk1) are defects with high contrast. In Fig. 23(a), (c) and (d), the results of B1, K1 and N1 are not satisfactory. In the next section, an improved version of the basic GIS method which can deal with these defects is given. The sample B1 (broken yarn) from the test images are commonly found in the process of weaving Jacquard. To provide more details, a sample is illustrated in Fig. 24.

5.1. Detection success rate on 60 samples using the GIS method

In this evaluation, a 10% noise level is assumed with the use of a 36×26 golden image. After the GIS process, the resultant images are 218×230, totally 50 140 pixels, 100 white pixels out of 50 140 (0.199%) are set as threshold for defective patterned image. All 30 defect-free images and 17 of 30 defective patterned images could be correctly detected after smooth filtering. The detection success rates are 100% for defect-free images and 56.67% for defective patterned images. Therefore, the overall success detection rate is 78.33%.

5.2. Effect due to noise levels in threshold images

As mentioned above, by assumption, there is a small amount of noise in the thresholded image D. So, noise should be eliminated in order to give the best result from defect detection. Fig. 25 shows that 10% noise level is the most appropriate level for test samples. If the noise level was adjusted to be too low, i.e. 1%, less result will be generated from defect detection. When the noise level is adjusted to 10%, the output would be satisfactory. However, the noise level could not be assumed too high. Otherwise, the threshold image would be in white color since the threshold value might reach the middle level of hills and valleys of resultant image.

5.3. Effect due to the size of golden image

Choosing a golden image is a key step for the basic GIS method. If the size is not bigger than or equal to a repetitive pattern, the detection would not be succeeded. Yet, if the size of golden image is bigger than a repetitive pattern, the result would be similar with those only approximately the same size of one repetitive pattern. Size in half (10×9), one (25×15), two (35×28) and five (47×40) repetitive units of golden image are tested and the size in 47×40 has given the best result. The results of choosing different

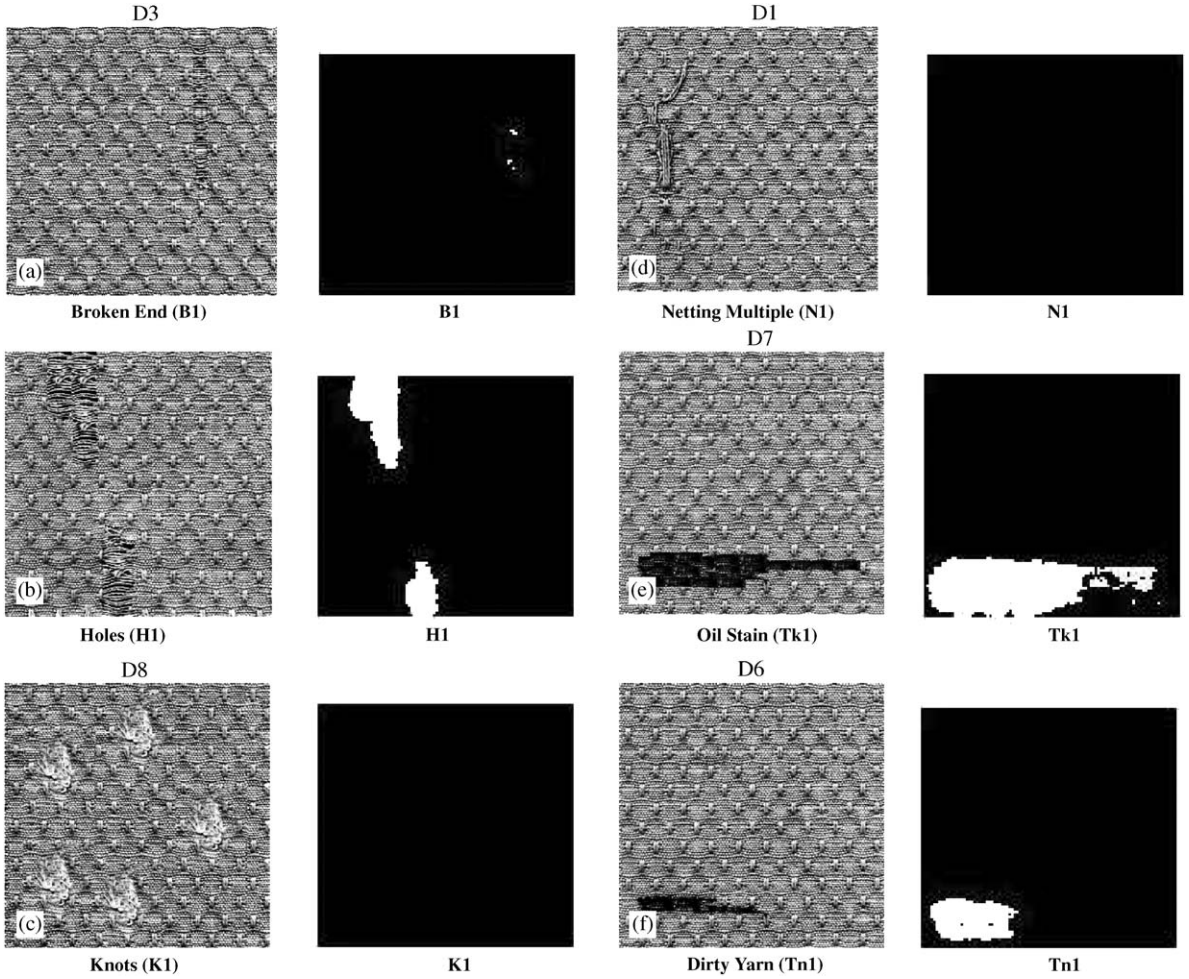

Fig. 23. Filtered six types of defective patterned images ((a) broken end, (b) holes, (c) knots, (d) netting multiple, (e) oil stain and (f) dirty yarn) with median filter of size [5 5].

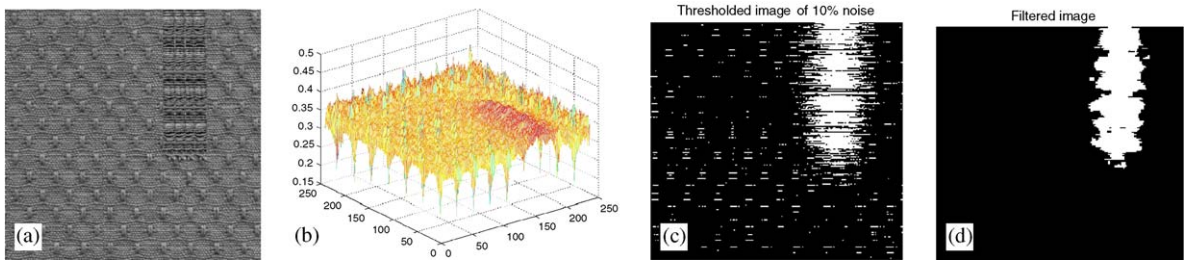

Fig. 24. (a) Histogram equalized test sample with broken yarn. (b) Mesh diagram after GIS, (c) threshold subtracted image, (d) Using median filter of size [5 5] on threshold image respectively.

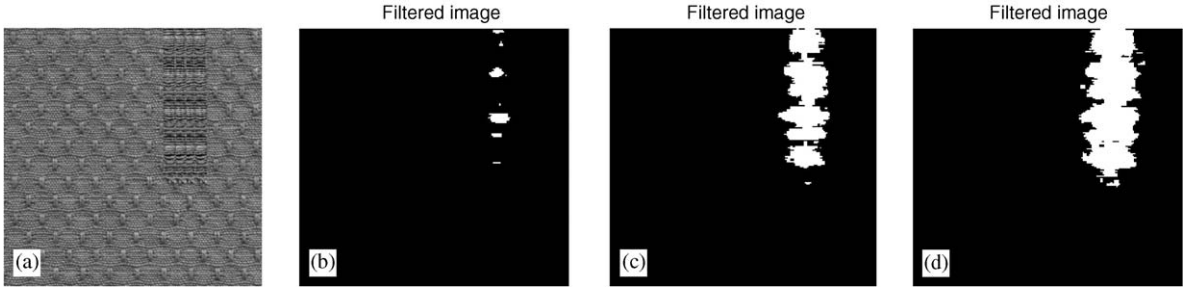

Fig. 25. (a) Histogram equalized test sample with broken yarn, (b) 1% noise, (c) 5% noise, (d) 10% noise in threshold image after using median filter.

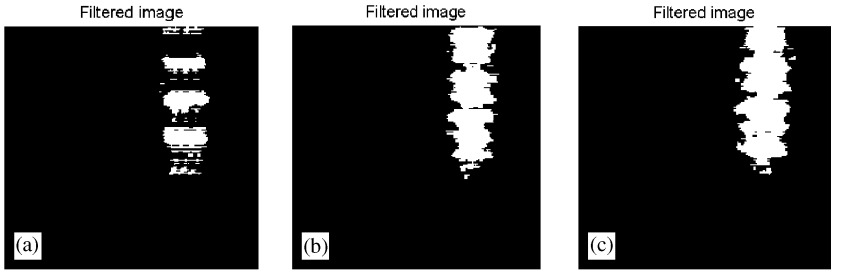

Fig. 26. Median filtering on thresholded image of pixel size (a) 25 × 15, (b) 35 × 28, (c) 47 × 40, golden images.

sizes of repetitive unit are shown in Fig. 26 for 10% noise thresholded image of broken yarn.

6. The wavelet preprocessed golden image subtraction (WGIS) method

In this section, WT preprocessed GIS method will be introduced (Fig. 27). With the inadequate results from the basic GIS method in the last section (Fig. 23), WGIS be shown to give a higher detection success rate.

6.1. The WGIS method

It is shown that noise on the patterned fabrics is a big obstacle for our detection method in last section. So, in order to tackle this problem, the basic GIS method has been improved and a new procedure is shown in Fig. 27. The WT, currently as a popular tool in image de-noising, image compression, segmentation [20,36–38], can be also considered as a preprocessing tool used to reduce the noise impulses in the test images.

The algorithm of WGIS method is developed to achieve a smoothing effect on the incoming histogram equalized image because there is often excessive noise on acquired image. During the step of WT, the first level *approximation* subimage by the Haar WT is extracted. This subimage of level 1 approximation is generated by passing through two low pass filters horizontally and vertically on the original image so that noise can be removed. Then, applying GIS on this approximated subimage would enhance the detection result.

In this method, the multiresolution and translation invariant properties are used and applied on the patterned fabric. After passing Haar WT to all images, the subimages in level 1 approximation of all images is selected which are of size 128 × 128. The resultant images after smooth filtering for defective patterned images are shown in Fig. 28. It is impressive that all six types of defective patterned images are detected. Twenty-eight out of 30 defect-free images are correctly detected. It should be noted that outlined regions correspond to the locations of the pattern defects.

6.2. Detection success rate on 60 samples using the WGIS method

A 10% noise level, a 36 × 26 golden image, first level approximation of the Haar WT are used in this part for 60 test images. After the WGIS process, the resultant images are 221 × 231, totally 51 051 pixels, 100 white pixels out of 51 051 (0.196%) are set as threshold for defective patterned image. Twenty-eight of 30 defect-free images and all 30 defective patterned images could be correctly detected after smooth filtering. The success detection rates are 93% for defect-free images and 100% for defective patterned images. Therefore, the overall success detection rate is 96.7%.

Fig. 27. The WT preprocessed GIS method.

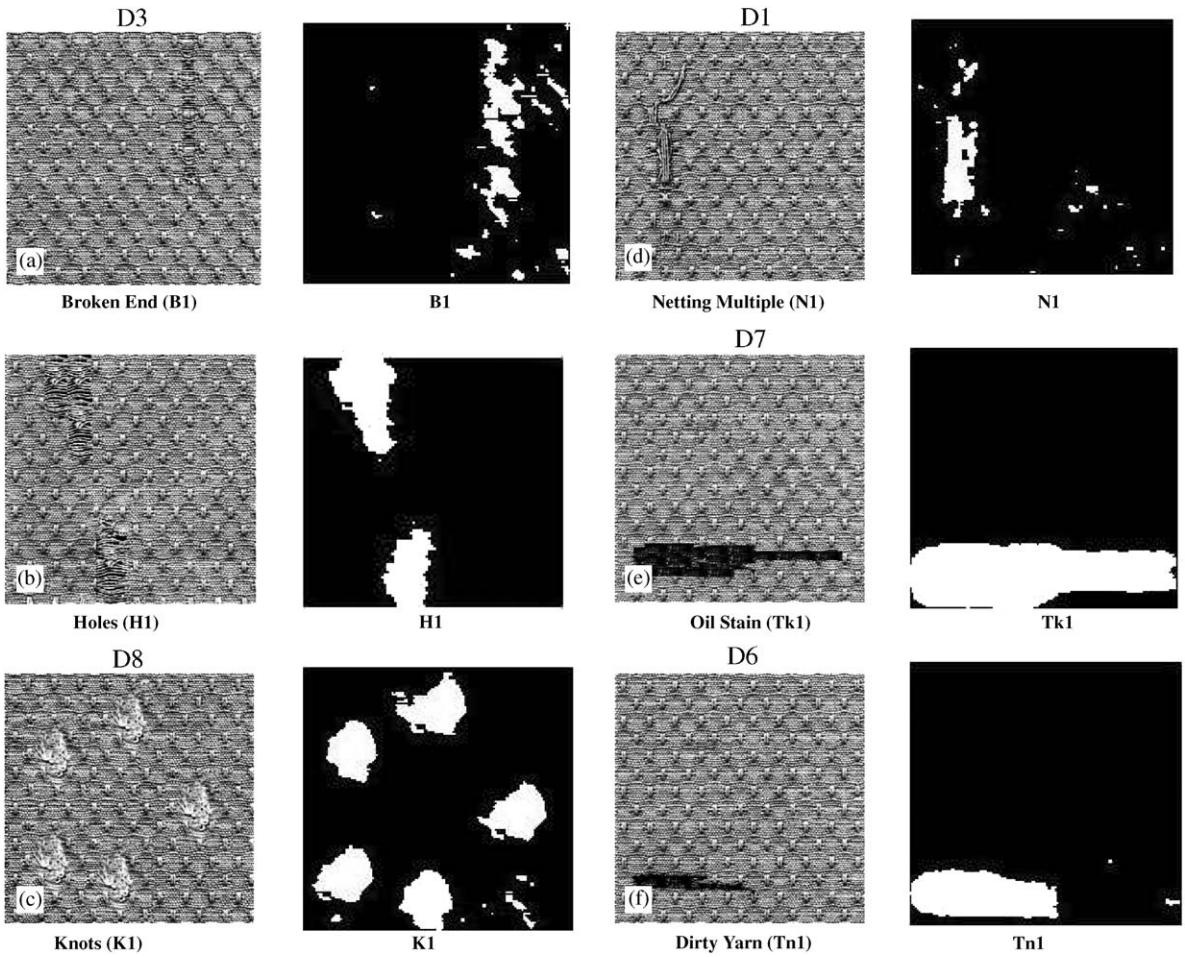

Fig. 28. Filtered six types of defective patterned images ((a) broken end, (b) holes, (c) knots, (d) netting multiple, (e) oil stain and (f) dirty yarn) with median filter of size [5 5].

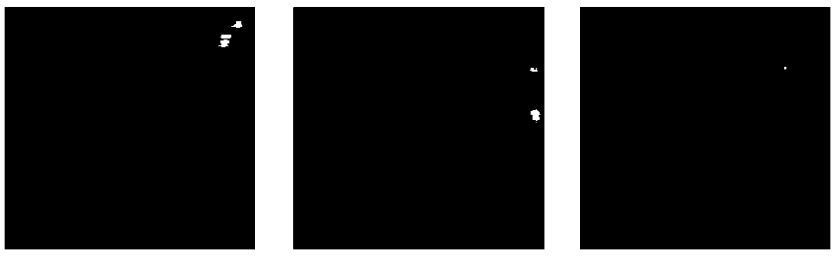

Fig. 29. Filtered four defective patterned images ((a) netting multiple, (b) dirty yarn, (c) oil stain and (d) knots) with median filter of size [15 15] in final step with excessive noise.

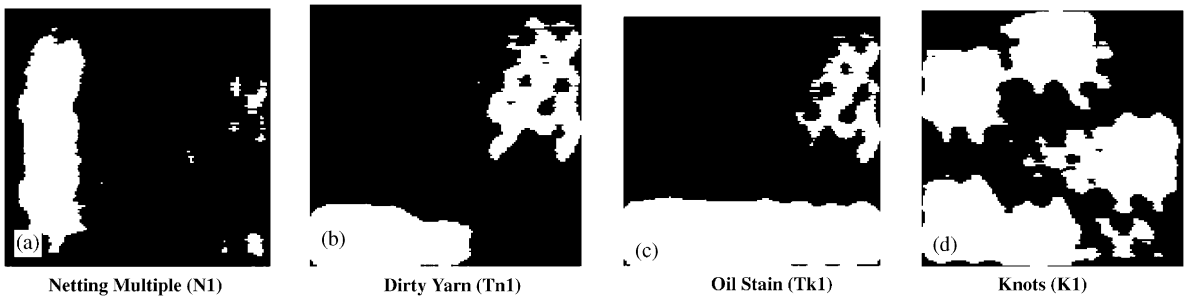

Fig. 30. Filtered three defect-free images with median filter of size [15 15] in final step.

60 test samples	Comparison of the Three methods		
	Method of DT on detailed subimages	The basic GIS method	The Wavelet Preprocessed GIS method
Successful Detected			
30 defect-free images	26	30	28
30 defective patterned images	27	17	30
Overall detection success rate	88.3%	78.33%	96.7%

Fig. 31. Comparison of detection success rate for the three main methods of this paper.

6.3. Effect due to using different 2D smoothing filters as preprocessing tool

Here, several 2D smoothing filters have been applied as pre-processing tool namely as Gaussian filter, averaging filter, wiener filter and median filter. The other steps are the same as before. The median filter in [3 3] is the most effective size to remove the impulse noise in the pre-processing step. It is impressive that all defective patterned images are detected but there are excessive noises found (Fig. 29). Also, the filtered defect-free images show some noises on them (Fig. 30). There is a need to eliminate such unwanted noises in order to lower the false positive rate.

7. Summary of the evaluation

In this paper, the DT method on detailed subimages, the basic GIS method and the wavelet preprocessed GIS method, have been evaluated with 60 test images. The results are shown in Fig. 31. Besides, the overall comment for all methods mentioned above are summarized in Fig. 32.

8. Conclusions

From the summary, it has been shown that the WGIS method provides the best detection result. The overall detection success rate is 96.7% with 30 defect-free images and 30 defective patterned images for one common kind of patterned Jacquard fabric.

The basic GIS method has several advantages. First, it can outline the shape of defect on patterned fabric. Secondly, the size of golden image can be easily chosen by the user. Thirdly, it does not have the alignment problem compared with the use of hash functions suggested by Bakyal [27,28]. Furthermore, the basic GIS method is different from the traditional subtraction method of Chin and Harlow [33] and Sandy [35]. They used exclusive-or operation to compare with one golden template and test image only, which would lead to alignment problem.

On the other hand, there are some weaknesses on the basic GIS method. Currently, the basic GIS method is effective for defect detection on the dot-patterned Jacquard since the contrast of this kind of patterned Jacquard is small enough and can be thresholded by $T_k = \max(r_{xy})$. For some extreme cases like using a charter-box patterned fabric with black and white color, the contrast would be very high and the defective region after the basic GIS method may not jump up higher than $T_k = \max(r_{xy})$. So, thresholding may not be so easy and this requires further research.

For the method of DT on detailed subimages, it shows 88.3% detection success rate for 60 test samples. With Haar wavelet decomposition, the method seems to be direct, effective and with low complexity when compared with the wavelet preprocessed GIS method. Although the wavelet preprocessed GIS method seems to have a higher complexity, it can detect defects with a finer shape and higher detec-

Method	Noise Level for threshold	Complexity	Comments for defect detection On dot-patterned Jacquard
Traditional Image Subtraction	-	Low	Not successful since too much noise exist in defect-free images
Hash function	-	Low since 1D approach	Not successful since it cannot outline the defective regions
Direct Thresholding	3%	Low but higher than hash function	Not successful
Basic GIS	10%	Higher than above	Not successful
Wavelet Preprocessed GIS	10%	Highest among all since it combine GIS and WT, but still low since the algorithm is simple and direct	*Successful*

Fig. 32. Overall comment of the three methods addressed in this paper.

tion success rate. Therefore, after comparing all methods in this paper, the wavelet preprocessed GIS method provides the most satisfactory result for defect detection on the dot-patterned fabric.

Acknowledgments

The supports from HKU CRCG of code 10205131, 10204488, 10205108, 7130/02P and 7046/03P are gratefully acknowledged.

References

[1] M. Bennamoun, A. Bodnarvova, Automatic visual inspection and flaw detection in textile materials: past, present and future, Proceedings of the IEEE Conference SMC, 1998, pp. 4340–4343.
[2] A. Bodnarova, M. Bennamoun, K.K. Kubik, Defect detection in textile materials based on aspects of HVS, Proceedings of the IEEE SMC' 98, Conference, San Diego, US, October 1998, pp. 4423–4428.
[3] C.H. Chan, H. Liu, T. Kwan, G. Pang, Automation technology for fabric inspection system, Proceedings of Conference on Applications of Automation Science and Technology, City University of Hong Kong, November 1998, pp. 24–26.
[4] G. Neubauer, Segmentation of defects in textile fabric, pattern recognition, Proceedings of IEEE 11th IAPR International Conference, Conference A: Computer Vision and Applications, vol.1, 30 August–3 September 1992, pp. 688–691.
[5] Y.F. Zhang, R.R. Bresee, Fabric defect detection and classification using image analysis, Text. Res. J. 65 (1995) 1–9.
[6] L.H. Hoffer, F. Francini, B. Tiribilli, G. Longobardi, Neural networks for the optical recognition of defects in cloth, Opt. Eng. 35 (1996) 3138–3190.
[7] J.G. Campell, A.A. Hashim, T.M. McGinnity, Flaw detection in woven textiles by neural network, Faculty of Informatics, Magee College, University of Ulster, Preprint INFM-97-002, May 1997.
[8] I.S. Tsai, C.H. Lin, J.J. Lin, Applying an artificial neural network to pattern recognition in fabric defects, Tex. Res. J. 65 (3) (1995) 123–130.
[9] C.H. Chan, G.K.H. Pang, Fabric defect detection by Fourier analysis, IEEE Tran. Ind. Appl. 36 (5) (2000).
[10] E.J. Wood, Applying Fourier and associated transforms to pattern characterization in textiles, Tex. Res. J. 60 (1990) 212–220.
[11] C. Castellinin, F. Francini, G. Longobardi, B. Tiribilli, On-line textile quality control using optical Fourier transforms, Opt. Lasers Eng. 24 (1996) 19–32.
[12] C. Cimberlini, F. Francini, G. Longobardi, P. Poggi, P. Sansoni, B. Tiribilli, Weaving defect detection by fourier imaging, Proc. SPIE 2786 (1996) 9–18.
[13] J.G. Campell, A.A. Hashim, F.D. Murtagh, Flaw Detection in Woven Textiles using Space-dependant Fourier Transform, Faculty of Informatics, Magee College, University of Ulster, Preprint INFM-97-004, May 1997.
[14] A. Kumar, G.K.H. Pang, Defect detection in textured materials using Gabor filters, IEEE Trans. Ind. Appl. 38 (2) (2002) 425–440.
[15] A. Kumar, G.K.H. Pang, Multi-channel defect segmentation using localized spatial filters, Opt. Eng. 39 (12) (2000) 3176–3190.
[16] A. Bodnarova, M. Bnnamoun, S. Lathm, Optimal Gabor filters for textile flaw detection, Pattern Recognition, J. Pattern Recognition Soc. 35 (2002) 2973–2991.
[17] D.M. Tsai, S.K. Wu, Automated surface inspection using gabor filters, Int. J. Adv. Manuf. Tech. 16 (2000) 474–482.
[18] A. Tilocca, Defecting fabric defects with a neural network using two kinds of optical patterns, Tex. Res. J. 72 (6) (2002) 545–551.
[19] G. Lambert, F. Bock, Wavelet methods for texture defect detection, 1997 Proceedings of International Conference

on Image Processing, vol. 3, 26–27, October 1997, pp. 201–204.
[20] A. Latif-Amet, A. Ertuzun, A. Ercil, An efficient method for texture defect detection: sub-band domain co-occurrence matrices, Image Vision Comput. 18 (1999) 543–553.
[21] H. Sari-Sarraf, J.S. Goddard, Vision System for On-Loom Fabric Inspection, IEEE Trans. Ind. Appl. 35 (6) (1999) 1252–1259.
[22] X.Z. Yang, G. Pang, N. Yung, Fabric defect classification using wavelet frames and minimum classification error training, IEEE 2002 37th IAS Industry Applications Conference Meetings, vol.1, 13–18 October 2002, pp. 290–296.
[23] Y.X. Zhi, G.K.H. Pang, N.H.C. Yung, Fabric defect detection using adaptive wavelet, Proceedings of 2001 IEEE ICASSP' 01 International Conference on Acoustics, Speech and Signal Processing, vol. 6, 7–11 May 2001, pp. 3697–3700.
[24] X. Yang, G.K.H. Pang, N. Yung, Discriminative fabric defect detection using adaptive wavelet, Opt. Eng. 41 (12) (2002) 3116–3226.
[25] A.L. Amet, A. Ertuzun, A. Ercil, Texture defect detection using subband domain co-occurrence matrices, IEEE Southwest Symposium on Image Analysis and Interpretation, April 1998, pp. 205–210.
[26] J.L. Dorrity, G.. Vachtsevanos, On-line defect detection for weaving systems, Proceedings of the IEEE Technical Conference on Textile, Fiber and Film Industry, 1996, pp. 1–6.
[27] I.C. Baykal, R. Muscedere, G.A. Jullien. On the use of hash functions for defect detection in textures for in-camera web inspection systems, IEEE International Symposium In Circuits and Systems, ISCAS 2002, vol. 5, 2002, pp. 665–668.
[28] I.C. Baykal, G.A. Jullien, Detection of defects in textures with alignment error for real-time line-scan web inspection systems, The 2002 45th Midwest Symposium In Circuits and Systems, 2002 MWSCAS, vol. 3, 2002, pp. 292–295.
[29] B. Kenneth, A note on the finite walsh transform, IEEE Trans. Inf. Theory 16 (4) (1970) 489–491.
[30] H. Schreiber, Bandwidth requirement for Walsh functions, IEEE Trans. Inf. Theory 16 (4) (1970) 491–493.
[31] K.R. Palanisamy, V.P. Arunachalam, Analysis of bilinear systems via single-term Walsh series, Int. J. Control 41 (2) (1985) 541–547.
[32] T. Thomas, M. Cattoen, Automatic inspection of simply patterned material in the textile industry, Proc. SPIE 2813 (1994) 2–12.
[33] R.T. Chin, C.A. Harlow, Automated visual inspection: a survey, IEEE Trans. Pattern Anal. Mach. Intell. PAMI-4 (6) (1982) 557–573.
[34] T. Li, P. Witty, K. Tim, Machine vision in the inspection on patterned textile webs, industrial inspection (Digest No:1997/041), IEE Colloquium, 10 February 97, pp. 9/1–9/5.
[35] C. Sandy, L. Norton-Wayne, R. Harwood, The automated inspection of Lace using machine vision, Mechatronics J. 5 (2/3) (1995) 215–231.
[36] R.C. Gonzalez, R.E. Woods, Digital Image Processing, 2nd ed., Prentice Hall, Englewood Cliff, NJ, 2002.
[37] D.M. Tsai, B. Hsiao, Automated surface inspection using wavelet reconstruction, Pattern Recognition 34 (2001) 1285–1305.
[38] S.G. Mallat, A Theory for multiresolution signal decomposition: the wavelet representation, IEEE Trans. Pattern Anal. Mach. Intell. 11 (7) (1989).

About the Author—HENRY Y.T. NGAN studied at The University of Hong Kong, HKSAR, China and received the B.Sc. (Mathematics) degree in 2001 and the M. Phil. (Electrical & Electronic Engineering) degree in 2004 respectively. He is currently working in the Industrial Automated Research Laboratory of the Department of Electrical and Electronic Engineering at The University of Hong Kong. His current research topic is Patterned Jacquard Fabric Defect Detection and his research interests include surface defect detection, image processing, pattern recognition and computer vision.

About the Author—DR. GRANTHAM K.H. PANG (http://www.eee.hku.hk/∼ gpang) obtained his Ph.D. degree from the University of Cambridge in 1986. He was with the Department of Electrical and Computer Engineering, University of Waterloo, Canada, from 1986 to 1996 and joined the Department of Electrical and Electronic Engineering at The University of Hong Kong in 1996. Since 1988, he published more than 130 technical papers and has authored or co-authored six books. He has also obtained two U.S. patents. His research interests include machine vision for surface defect detection, optical communications, expert systems for control system design, intelligent control and intelligent transportation systems. Dr. Pang is in charge of the Industrial Automation Research Lab (http://www.eee.hku.hk/∼gpang/IARL/HomeIARL.htm). Dr. Pang has acted as a consultant to many companies, including Mitsubishi Electric Corp. in Japan, Northern Telecom and Imperial Oil Ltd. in Canada, MTR Corp. and COTCO Int. Ltd. in Hong Kong. In 1994, he worked as a Senior Visiting Researcher at Hitachi Research Lab. in Japan. Dr. Pang is a Chartered Electrical Engineer, and a member of the IEE, HKIE as well as a Senior Member of IEEE.

About the Author—DR. MICHAEL K. NG was born in Hong Kong, China, in 1967. He received B. Sc. and M. Phil. degrees in Mathematics from the University of Hong Kong, in 1990 and 1993, respectively, and Ph.D. degree in Mathematics from the Chinese University of Hong Kong, in 1995. From 1995 to 1997 he was a Research Fellow at the Australian National University. He is an Associate Professor in the Department of Mathematics at the University of Hong Kong. Ng's research interests are in the areas of data mining, operations research and scientific computing. He has been selected as one of the recipients of the Outstanding Young Researcher Award of the University of Hong Kong in 2001. He is currently on the editoral board of the journals "Numerical Linear Algbera with Applications", "Numerical Mathematics", "Multidimensional Systems and Signal Processing" and "Journal of Computational Science and Engineering".

About the Author—DR. S.P. YUNG obtained his Ph.D. degree from the University of Wisconsin-Madison in 1991 and joined the Department of Mathematics, University of Hong Kong since then. His interests are in system and control theory. He also got attracted to wavelets and is testing some applications with them.